Journal of Sensor Science and Technology
Vol. 34, No. 1 (2025) pp. 37-43
http://dx.doi.org/10.46670/JSST.2025.34.1.37
pISSN 1225-5475/eISSN 2093-7563

Research on an Electrochemical Salinity Sensor with Indium-Tin-Oxide Conductive Ceramic Electrodes

Chanyoung Bae[1], Mincheol Han[1], Yujin Song[1], Hyunjun Lee[1], Moonjin Lee[2], Jae-Jin Park[2], and Jiho Chang[1,+]

Abstract

Salinity is a critical metric in aquatic environmental monitoring because it can fluctuate owing to water pollution or the presence of harmful substances. In this study, a salinity sensor based on a conductive ceramic film made of indium tin oxide (ITO) is proposed to address the issues of contamination and corrosion commonly observed in conventional salinity sensors that use metal electrodes. By improving the operational stability and measurement reliability, the proposed sensor offers a robust alternative for salinity monitoring. The sensor was fabricated using an efficient semiconductor process, comprising two quartz substrates with the ITO film deposited on them in a facing configuration. The salinity levels were varied from 30 to 40 practical salinity units (PSU), and the sensor was tested under both direct and alternating currents to evaluate the changes in conductive resistance and impedance between the electrodes. The resistance changes exhibited strong linearity with an average correlation coefficient exceeding 0.97, confirming that the proposed sensor is feasible for salinity monitoring applications.

Keywords: Environmental monitoring, Salinity sensor, Electrochemical sensor, ITO (Indium-Tin-Oxide)

1. INTRODUCTION

Salinity is an important indicator of water quality and its measurement plays a crucial role in various fields, including aquatic environmental monitoring, agriculture, and water management [1,2]. Salinity sensors measure salt concentrations using various principles, each with distinct features, advantages, and limitations. These sensors can be broadly categorized as follows.

Density-based salinity sensors measure the density of water to determine its salinity. However, their complexity and relatively slow response time render them unsuitable for portable devices [3]. Refractive-index-based salinity sensors determine salinity by measuring the refractive index of light in water. They provide relatively high-precision measurements and are less affected by environmental changes [4]. However, their reliance on complex equipment for accurate refractive-index measurements makes them expensive. Potentiometric salinity sensors use ion-selective electrodes to measure potential differences in response to specific ion concentrations. Despite their usefulness, these sensors require periodic calibration and are prone to interference from other ions [5]. Optical salinity sensors are based on the absorption or scattering of specific wavelengths of light depending on salinity [6]. Although highly accurate and with fast response times, they rely on optical components, which make them expensive and less effective in turbid underwater environments.

Consequently, conductivity-based salinity sensors, which are portable, economical, and maintenance-free, are attracting growing interest. These sensors leverage the fact that water conductivity increases with salinity. They have relatively simple structures and allow quick measurements with short reaction times. However, their performance is influenced by factors such as the type of ions in the water and temperature. Therefore, additional research is required to ensure accurate and reliable measurements.

A significant challenge faced by conductivity-based salinity sensors is the corrosion of the metal electrodes, which shortens the sensor lifespan and reduces measurement reliability. Although chemical sensors enable contactless measurements, they are often complex, expensive, and only accurate under specific conditions [7]. These limitations underscore the need for new salinity sensors with improved performance and cost-effectiveness.

Indium tin oxide (ITO) is a metal oxide that is more corrosion-

[1]Major of Nano-Semiconductor Engineering, Korea Maritime and Ocean University (KMOU), Busan 49112, Korea
[2]Maritime Safety and Environment Research Center, Korea Research Institute of Ship & Ocean Engineering, Daejeon 34103, Korea
[+]Corresponding author: jiho_chang@kmou.ac.kr
(Received: Dec. 18, 2024, Revised: Jan. 1, 2025, Accepted: Jan. 13, 2025)

resistant than metals and is widely used in various fields owing to its high reliability. In particular, ITO is utilized as a transparent electrode material owing to its excellent electrical properties, optical transmittance, and high environmental stability and is attracting attention as a reliable material for various sensors and electronic devices [8].

In this study, we utilized these properties of ITO to overcome the limitations of existing salinity sensors. In particular, an electrochemical salinity sensor based on the conductive ceramic ITO was developed to solve the problems of electrode corrosion and fouling, extend the sensor lifetime, and increase cost-effectiveness. The sensor, realized through a simple process, was evaluated for its operational performance over a wide range of salinities under DC and AC biases, confirming its potential to overcome the shortcomings of existing technologies and enable more reliable salinity measurements.

2. EXPERIMENTAL

In this study, conductive ceramics were used as electrodes to fabricate a sensor that detected changes in conductivity caused by variations in liquid salinity. Fig. 1 (a)–(f) show the fabrication process of the sensor. Fig. 1 (a) shows a quartz substrate with ITO deposited on it. It measures 25 mm × 75 mm × 1.1 mm, and ITO was deposited on top of it at a thickness of 30 nm. Fig. 1 (b) shows the cleaning process of the substrate. The substrate was immersed in deionized ionized (DI) water using a cleaning carrier and cleaned in an ultrasonic cleaner for 6 min to remove any contamination present on its surface. After cleaning, a nitrogen (N2) gas gun was used to remove any residual moisture from the surface. Fig. 1 (c) shows the pre-baking process performed prior to PR coating. In this step, the surface of the substrate was heat treated at 90°C for 60 s to ensure good bonding between the substrate and PR. Prebaking removed any remaining moisture from the surface of the substrate and ensured that the PR was uniformly applied to the substrate. AZ GXR-601 was used as the PR for coating. Fig. 1 (d) shows the process of applying the PR to the substrate using a spin coater at 6000 RPM for 60 s. Fig. 1 (e) shows the post-baking process after PR coating. In this step, the PR is further annealed at 90°C for 60 s to strengthen the bond between the PR and substrate and increase the hardness of the PR layer. Fig. 1 (f) shows the final state of the substrate with a uniformly coated PR.

Fig. 1 (g) presents a schematic of the sensor structure. The schematic illustrates the arrangement of the two ITO substrates,

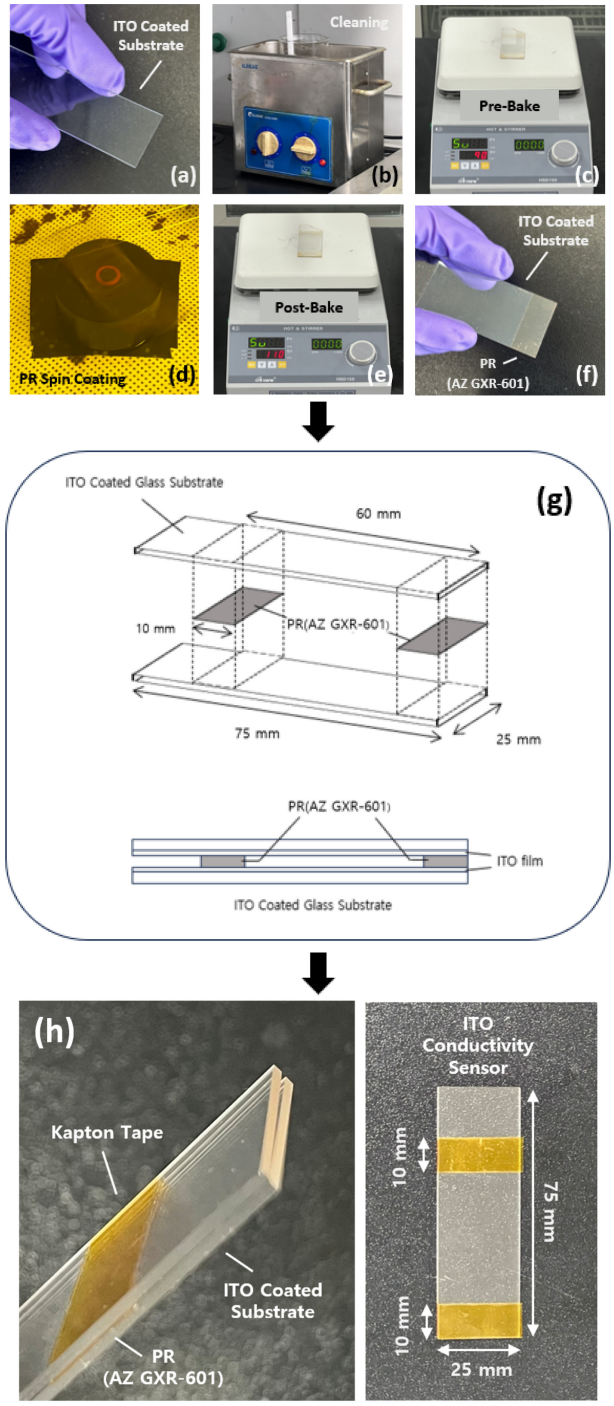

Fig. 1. (a)–(f) Photographs illustrating the fabrication process of sensors with ITO-coated substrates. (g) Schematic of the sensor structure. (h) Photographs showing the sensor shape.

the PR spacer that determines the gap between the electrodes, and the exposed ITO layer at the top edge of the electrode for instrument connections. The alignment of the conductive ITO layers and application of Teflon tape to secure the substrates are also highlighted in this diagram.

Fig. 1 (h) illustrates the structure of the sensor constructed using

commercially available ITO substrates. The two ITO substrates were aligned with their conductive ITO layers facing each other, with a PR spacer positioned between the two faces. The thickness of the PR spacer was 2.1 μm, which determined the gap between the two electrodes. To secure the two ITO substrates, a Teflon tape was employed because of its chemical stability and suitability for identifying the chemical properties of the liquids. Additionally, to enable connections of the measurement instrument and facilitate sensor performance evaluation, a triangular area measuring 15 mm× 15 mm was removed from the top edge of each electrode, exposing the underlying ITO layers.

To evaluate the change in conductivity between the electrodes owing to salinity variations, the resistance and impedance changes were measured under DC and AC biases, respectively. The two electrodes were immersed in 400 mL of an analyte prepared by diluting DI water with sodium chloride (NaCl) to a predetermined depth of 12.5 mm. The salinity range was varied between 30 and 40 PSU with a measurement interval of 2.5 PSU. As a reference, 1 PSU corresponds to a salinity of approximately 0.1%. Thus, salinity levels of 30 and 40 PSU correspond to 3.0% and 4.0% salt concentrations, respectively. These salinity ranges are representative of typical marine environments, making them suitable for evaluating the sensor's performance [9].

3. RESULTS AND DISCUSSIONS

3.1 Optimizing Bias Conditions for Salinity Sensor

To evaluate the performance of a conductive salinity sensor, it is essential to establish the appropriate bias conditions. The most critical reason is to prevent electrolysis between the electrodes, which occurs at voltages exceeding 1.2 V, the electrolysis voltage of water. Furthermore, some studies have recommended a voltage of 0.8 V or less to avoid chlorination reactions on the electrode surface [10]. In this study, the optimal bias voltage for the salinity sensor with ceramic electrodes was determined based on these considerations.

Fig. 3 shows the results of immersing the sensor in a brine solution with a salinity of 40 PSU at a depth of 12.5 mm, while varying the bias voltage from 0.2 to 1.2 V in 0.2 V increments. Below 0.6 V, the resistance remained constant, whereas above 0.8 V, the resistance decreased linearly with increasing bias voltage.

Section (a) of Fig. 3 illustrates the rate of resistance change for bias voltages ranging from 0.2 to 0.6 V, with a slope of (ΔR/ΔV) = 0.27 kΩ/V. In this range, the resistance change was negligible,

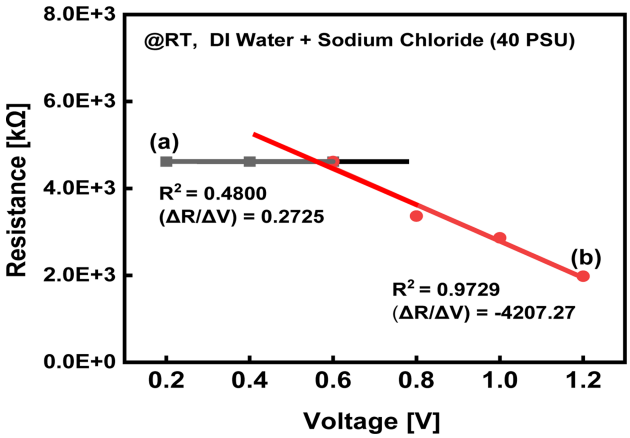

Fig. 2. Resistance response of the salinity sensor in two bias voltage ranges: (a) 0.2–0.6 V and (b) 0.8–1.2 V.

indicating that the performance of the sensor was stable and the risk of water electrolysis was minimized. In contrast, section (b) of Fig. 3 presents the results for bias voltages between 0.8 and 1.2 V, where the resistance decreased linearly, with a slope of (ΔR/ΔV) = −4207.3 kΩ/V (R^2 = 0.97 for the trend line).

According to Lu et al. [11], the decrease in resistance with increasing bias voltage can be attributed to the enhanced interaction between the electrode and electrolyte. In brackish water, a chlorination reaction occurs, leading to a decrease in the observed resistance. Specifically, at voltages above 0.8 V, chloride ions (Cl^-) react with the electrode surface, causing a rapid increase in conductivity and a corresponding linear decrease in resistance. Based on these findings, a bias voltage of 0.6 V was selected as the optimal condition for the salinity sensor. This choice ensured that the sensor remained within a stable resistance range, while preventing electrolysis and chlorination reactions at the electrode surface.

3.2 Salinity Sensor Characterization under DC Bias

Fig. 3 (a) shows the results of placing the ITO sensor in contact with the liquid analyte at a certain depth and recording the change in resistance over time at a direct current (DC) bias voltage. Prior to immersion in the analyte, the sensor exhibited a large resistance because of the open circuit between the two electrodes; however, a sharp decrease in resistance was observed immediately after the sensor was immersed in the analyte. This is due to the physical and electrochemical properties of the ITO surface. As a semiconductor, ITO is subjected to charge redistribution at the semiconductor/liquid interface when in contact with a liquid. When there is a difference between the electrochemical potential

of the solution and the Fermi level of ITO, charges move across the interface to form an equilibrium state, which results in an initial decrease in the resistance [12].

In particular, as the concentration of salt (e.g., NaCl) in the analyte increases, the conductivity of water increases, and ionic migration and charge transfer become more active, resulting in a significant decrease in resistance. However, an increase in the resistance was observed over time, which can be explained by ion adsorption and rearrangement on the ITO surface and charge screening effects. Initially, the ions in water are rapidly adsorbed on the ITO surface, increasing the conductivity; however, over time, the active sites of the adsorbable surface become saturated [13].

During this process, the resistivity increases slowly as the charge density on the surface changes or a dynamic equilibrium of ions is established [14]. After approximately 5.3 s, electrochemical equilibrium was established between the ITO surface and the solution, and the resistance reached a constant saturation state.

Fig. 3 (b) shows the variation in the saturation resistance values with salinity, as shown in Fig. 3 (a). As salinity increased, the resistivity decreased linearly, indicating a corresponding increase in conductivity. Salinity reflects the concentration of ions dissolved in water. Higher salinity increases ion concentration, enhances ionic conduction, and consequently reduces resistance [15]. Quantitatively, electrical conductivity (σ) is inversely related to resistance (R), which can be expressed by the following equation [15]:

$$\sigma = L/(R \cdot A) \tag{1}$$

Here, σ represents conductivity in siemens per centimeter, R is the resistance in ohms, A is the cross-sectional area of the current path in square centimeters, and L is the length of the current path in centimeters. Additionally, a relationship exists between ion concentration (C) and conductivity, as shown in the following equation [16]:

$$\sigma = \Lambda_m \cdot C \tag{2}$$

In this equation, Λ_m represents molar conductivity in siemens square centimeters per mole, and C is the ion concentration in moles per liter. This relationship explains why increasing salinity leads to a higher C value, which enhances conductivity and consequently reduces resistivity [15,16].

Based on the data in Fig. 3 (b), the relationship between the salinity (S) and resistance (R) can be quantitatively defined. The data measured in this study showed that the change in resistivity

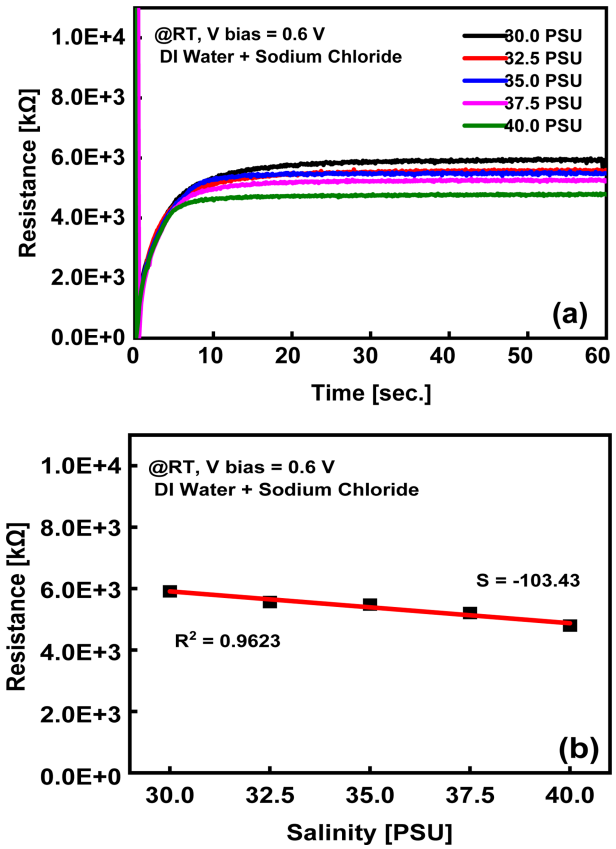

Fig. 3. Resistance characterization of the salinity sensor: (a) Time-dependent resistance change at a DC bias voltage and (b) saturation resistance variation with salinity

as a function of salinity can be represented as a linear function. The forward transfer function is defined as

$$R(S) = k \cdot S + R_0 \tag{3}$$

In this equation, k represents the slope or sensitivity of the transfer function in ohms per PSU, calculated as $(\Delta R/\Delta S) = -103.4\ \Delta k\Omega/\Delta PSU$. R_0 is the resistance when the salinity is 0 PSU, which was calculated as $R_0 = 9011.7\ k\Omega$. Using this transfer function, the performance of the salinity sensor with ceramic electrodes can be mathematically modeled as

$$S = (R - R_0)/k \tag{4}$$

This equation enables real-time salinity prediction based on resistance measurements. The data in Fig. 3 (b) demonstrate high linearity with an R^2 value of 0.96, confirming that the transfer function is a reliable model for salinity measurement. This high linearity minimizes the impact of measurement errors, such as temperature changes or electrode surface contamination, especially when measured under controlled laboratory conditions [17].

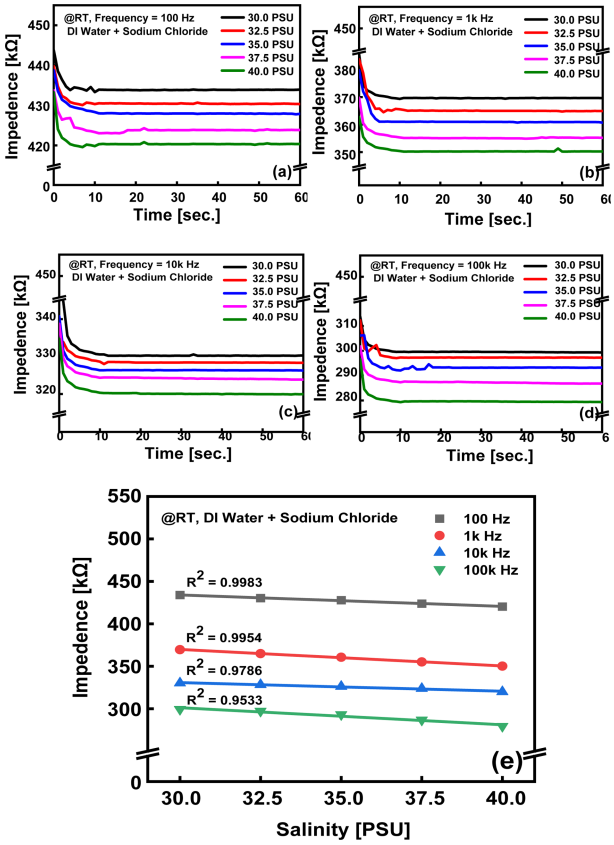

Fig. 4. Impedance characterization of the salinity sensor under AC bias conditions: (a)–(d) Time-dependent impedance changes at varying frequencies. (e) Saturation impedance values as a function of salinity and frequency.

3.3 Salinity Sensor Characterization under AC Bias

The sensor was further characterized using an alternating current (AC) bias voltage. Although DC-bias voltage-based measurements are simple in structure and easy to perform, they are prone to chemical reactions and electrochemical interference at the electrode surface [18]. In contrast, AC bias voltages minimize this interference and enable the use of high-frequency signals, resulting in more sensitive and reliable measurements [19].

Fig. 4 (a)–(d) illustrate measurements obtained under AC bias conditions. The sensor was immersed in the analyte to a specific depth, and the peak amplitude of the alternating voltage (V_{peak}) was limited to 0.6 V. The frequency was varied from 100 Hz to 100 kHz and the impedance changes over time were recorded. Before immersion in the analyte, the two electrodes were open and exhibited a high impedance. Upon immersion in the liquid analyte, the impedance initially decreased and then saturated at a specific value. On average, this saturation occurred within 5 s.

Fig. 4 (e) shows the variation in the saturation impedance values with salinity as a function of frequency, as described in Fig. 4 (a)–(d). Similar to the measurements under a DC bias, the impedance values decreased linearly with increasing salinity (indicating an increase in conductivity). This behavior can be explained by the relationship between impedance and resistance [20]:

$$Z = R + jX \tag{5}$$

where Z is the impedance (Ω), R is the resistance (Ω), and X is the reactance, which represents the frequency-dependent component that impedes current flow. The relationship with Equation (1) is as follows:

$$Z = \sqrt{(R^2 + X^2)} \tag{6}$$

The decrease in impedance with increasing salinity can be explained considering the relationship between Equations (6) and (2). Similarly, based on the data shown in Fig. 5 (e), the relationship between salinity (S) and impedance (Z) can be quantitatively defined. The data obtained in this study indicate that the change in impedance with salinity can be represented as a linear function. The transfer function is defined as follows:

$$Z(S) = k' \cdot S + Z_0 \tag{7}$$

$$S = (Z - Z_0)/k' \tag{8}$$

where Z(S) is the impedance at a specific salinity, k′ is the impedance change rate (ΔZ/ΔS), and Z_0 is the impedance at salinity 0 PSU. From the experimental results, k′ = −1.43 (ΔZ/ΔS) and Z_0 = 474.3 kΩ were obtained at a frequency of 100 Hz. The highest linearity was achieved with R^2 = 0.99, confirming that the AC-voltage-based impedance measurements provide a reliable model to accurately reflect changes in salinity.

Brett et al. [19] demonstrated that alternating current measurements offer higher accuracy because they can separate the effects of capacitance and reactive resistance, depending on the frequency conditions. Among electrode-type sensors, especially when the electrodes have a large area, capacitive effects due to the accumulation of charge on the electrode surface are known to occur, thereby affecting the measurement accuracy. Therefore, measurements under an AC bias were preferred [20]. In particular, in the low-frequency region, the response at the electrode–electrolyte interface became significant, with resistive elements related to ion diffusion and migration serving as the main contributors. Under these conditions, the difference in impedance with changes in salinity was relatively large and the change in conductivity was clearly reflected, resulting in a high degree of linearity.

However, in the high-frequency region, the capacitance effects dominated. The complex reactions at the electrode interface were reduced, and ion migration was less influential. As a result, the impedance change at high frequencies was relatively small compared to that at low frequencies. This effect is predicted to increase when the sensor is operated in an environment containing a variety of interacting water ions, such as seawater. However, we found that the relationship between salinity and impedance still exhibited a high degree of linearity in the low-frequency region with the AC voltage. This relationship can be effectively utilized to predict the salinity in real time.

These results demonstrate that the salinity sensor developed in this study has the potential to provide reliable data in various environments.

4. CONCLUSIONS

In this study, a salinity sensor with ITO ceramic electrodes was fabricated using a simple process. To evaluate the performance of the salinity sensor, its response to changes in bias conditions was analyzed. It was confirmed that a bias voltage above 0.8 V leads to chlorine reactions, which reduce measurement accuracy. Therefore, 0.6 V was identified as the optimal bias voltage.

Under DC bias conditions, the sensitivity was determined to be $(\Delta R/\Delta S) = -103.4\ \Delta k\Omega/\Delta PSU$ with $R^2 = 0.96$. Under AC bias conditions at a frequency of 100 Hz, the sensitivity was $(\Delta Z/\Delta S) = -1.34\ \Delta k\Omega/\Delta PSU$ with $R^2 = 0.99$, indicating that these conditions are the most suitable for operation. These findings demonstrated the feasibility of using ITO ceramic electrodes in conductive salinity sensors.

Aquatic environments often contain not only salts but also various biomolecules, such as proteins and fats, as well as pollutants, such as heavy metals and fine particles. These substances can significantly influence the sensor performance. To address this issue, future research will focus on systematically analyzing the complex effects of these substances on sensor signals [21].

To enhance the selectivity and reliability of ITO-based sensors, we will explore their integration with complementary technologies, such as optical or electrochemical sensors, to enable the simultaneous detection of multiple contaminants. For example, optical sensor integration can differentiate between salinity and biomolecular interference by using fluorescence or spectroscopic methods.

Furthermore, we plan to design physical or chemical pretreatment devices to reduce non-specific signals, such as ion adsorption or biomolecule interference, to improve the sensor accuracy in complex environments. These devices can include filters for particulate matter or chemical coatings to selectively block interfering substances.

These advancements aim to significantly improve the performance of ITO-based salinity sensors and broaden their applicability in environmental monitoring and water quality assessment. By addressing the challenges posed by real-world underwater environments, this research contributes to the development of more robust and reliable sensor technologies.

ACKNOWLEDGMENT

This research was supported by the Korea Institute of Marine Science & Technology Promotion (KIMST) funded by the Ministry of Oceans and Fisheries, Korea (RS-2021-KS211535, ‘Development of Technology for Impact Assessment and Management of HNS discharged from Marine Industrial Facilities’).

REFERENCES

[1] R. R. Shamshiri, S. K. Balasundram, A. K. Rad, M. Sultan, and I. A. Hameed, *“An Overview of Soil Moisture and Salinity Sensors for Digital Agriculture Applications,” in Digital agriculture, methods and applications,* R. R. Shamshiri and Sanaz Shafian, Eds. IntechOpen, London, pp. 1-166, 2022.

[2] J.-Y. Lin, H.-L. Tsai, and W.-H. Lyu, “An Integrated Wireless Multi-Sensor System for Monitoring the Water Quality of Aquaculture”, *Sens.*, Vol. 21, No. 24, p. 8179, 2021.

[3] A. N. Grekov, N. A. Grekov, and E. N. Sychov, “Measuring Salinity and Density of Seawater Samples with Different Salt Compositions and Suspended Materials”, *Metrol.*, Vol. 1, No.2, pp. 107-121, 2021.

[4] G. Li, Y. Wang, A. Shi, Y. Liu, and F. Li, “Review of Seawater Fiber Optic Salinity Sensors Based on the Refractive Index Detection Principle”, *Sens.*, Vol. 23, No. 4, p. 2187, 2023.

[5] https://en.wikipedia.org/wiki/Ion-selective_electrode (retrieved on Dec. 15, 2024).

[6] L. Zhou, Y. Yu, H. Huang, Y. Tao, K. Wen, G. Li, J. Yang, and Z. Zhang, “Salinity Sensing Characteristics Based on Optical Microfiber Coupler Interferometer”, *Photonics*, Vol. 7, No. 3, p. 77, 2020

[7] X. Wang, X. Bai, M. Zhang, and C. Wu, “High-Resolution Seawater Salinity Sensor Based on Temperature Self-Compensating Optical Interferometer”, *IEEE Sens. J.*, Vol. 24, No. 2, pp. 1374-1382, 2024.

[8] S.-H. Lee, S.-M. Cho, C.-M. Kim, H.-H. Kim, H.-U. Yang, J.-E. Oh, and J.-H. Chang, "A Study on the fabrication of HNS remote sensor module with printed ITO films", *J. Adv. Mar. Eng. Technol.*, Vol. 40, No. 4, pp. 325-329, 2016.
[9] https://opencontent.ccbcmd.edu/ccardona2023oceanography/chapter/5-3-salinity-patterns/ (retrieved on Dec. 15, 2024).
[10] A. A. Gewirth and B. K. Niece, "Electrodeposition of ZnO Films and their Conversion to Nanowires", *J. Electroanal. Chem*., Vol. 66, No. 6, pp. 1-7, 2010.
[11] S.-H. Lu, Y. Li, and X. Wang, "Soft, flexible conductivity sensors for ocean salinity monitoring", *J. Mater. Chem. B*, Vol. 11, No. 31, pp. 7334-7343, 2023.
[12] S. An, J. Noh, C. Lee, S. Lee, D. Seo, M. Lee, and J. Chang, "Study on the Effect of the Electrode Structure of an ITO Nanoparticle Film Sensor On Operating Performance", *J. Sens. Sci. Technol.*, Vol. 31, No. 2, pp. 90-95, 2022.
[13] S. Dasgupta, M. Lukas, K. Dössel, R. Kruk, and H. Hahn, "Electron mobility variations in surface-charged indium tin oxide thin films", *Phys. Rev. B*, Vol. 80, No. 8, p. 085425, 2009.
[14] Z. X. Chen, Y. J. Xi, L. Huang, W. C. Li, R. Li, G. Q. Xu, and H. S. Cheng, "A novel surface modification scheme for ITO nanocrystals by acetylene: a combined experimental and DFT study", *Phys. Chem. Chem. Phys.*, Vol. 17, No. 40, pp. 26728-26736, 2015.
[15] H. S. Magar, R. Y. A. Hassan, and A. Mulchandani, "Electrochemical Impedance Spectroscopy (EIS): Principles, Construction, and Biosensing Applications", *Sens.*, Vol. 21, No. 19, p. 6578, 2021.
[16] N. O. Laschuk, E. B. Easton, and O. V. Zenkina, "Reducing the resistance for the use of electrochemical impedance spectroscopy analysis in materials chemistry", *RSC Adv.*, Vol. 11, No. 45, pp. 27925-27936, 2021.
[17] https://szphoton.com/ko/blogs/articles/what-does-linearity-mean-in-sensors?utm_source(retrieved on Jan. 9, 2025)
[18] Y. Li, L. Wang, and X. Zhang, "Effects of DC bias voltage on electrochemical sensors: Reaction mechanisms and performance evaluation", *J. Electrochem. Sci. Technol.*, Vol. 22, No. 3, pp. 185-193, 2020.
[19] C. M. A. Brett, "Electrochemical Impedance Spectroscopy in the Characterisation and Application of Modified Electrodes for Electrochemical Sensors and Biosensors", *Molecules*, Vol. 27, No. 5, p. 1497, 2022.
[20] O. Khaldi, F. Jomni, P. Gonon, and C. Vallée, "AC and DC bias effect on capacitance–voltage nonlinearities in Au/HfO?/M (M=Pt, TiN, W, and AlCu) MIM capacitors: effect of the bottom electrode material," *J. Mater. Sci. Mater. Electron.*, Vol. 31, pp. 19036-19043, 2020.
[21] https://en.wikipedia.org/wiki/Electrical_impedance? (retrieved on Dec. 15, 2024).
[22] J. Jeon, S. An, C. Lee, Y. Cho, C. Bae, D. Kim, Y. Song, M. Han, J. Chang, Y. Ha, J. Park, and M. Lee, "A Study on the Application of Underwater Metal Ion Detection Sensor Using ITO Nanoparticle Printed Thin Film", *New Phys. Sae Mulli*, Vol. 74, No. 1, pp. 107-112, 2024.